Synthesis, Characterization, Photoinduced Isomerization, and Spectroscopic Properties of Vinyl-1,8-naphthyridine Derivatives and Their Copper(I) Complexes

Wen-Fu Fu,*,†,‡ Lin-Fang Jia,† Wei-Hua Mu,‡ Xin Gan,‡ Jia-Bing Zhang,‡ Ping-Hua Liu,‡ Qian-Yong Cao,† Gui-Ju Zhang,† Li Quan,† Xiao-Jun Lv,† and Quan-Qing Xu‡

†*Key Laboratory of Photochemical Conversion and Optoelectronic Materials, HKU-CAS Joint Laboratory on New Materials, Technical Institute of Physics and Chemistry, Chinese Academy of Sciences, Peking 100190, China, and* ‡*College of Chemistry and Chemical Engineering, Yunnan Normal University, Kunming 650092, China*

Received January 16, 2010

A series of 1,8-naphthyridine derivatives containing vinyl, 2-(2-acetylamino-pyridine-6-ethylene)-4-methyl-7-acetylamino-1,8-naphthyridine (**L^1**), 2-(2-acetylamino-pyridine-6-ethylene)-1,8-naphthyridine (**L^2**), 2-(2-acetylamino-pyridinyl-6-ethylene)-4-methyl-7-hydroxyl-1,8-naphthyridine (**L^3**), 2-(2-diacetylamino-pyridinyl-3-ethylene)-7-diacetylamino-1,8-naphthyridine (**L^4**), and 7-(2-diacetylamino-pyridinyl-3-ethylene)-4′-acetyl-pyrrolo[1′,5′-*a*]-1,8-naphthyridine (**L^5**), as well as complexes [CuL^1(PCy$_3$)](BF$_4$)$_2$ (**1**) (PCy$_3$ = tricyclohexylphosphine), [Cu$_2$L^1(PPh$_3$)$_4$](BF$_4$)$_2$ (**2**) (PPh$_3$ = triphenylphosphine), [Cu$_2$L^1(dppm)](BF$_4$)$_2$ (**3**) (dppm = bis(diphenylphosphino)methane), and [Cu$_2$L(^{1})(dcpm)][BF$_4$]$_2$ (**4**) (dcpm = bis(dicyclohexylphosphino)methane, were synthesized. All these compounds, except for **L^1** and **L^2**, were characterized by single crystal X-ray diffraction analysis, and a comprehensive study of their spectroscopic properties involving experimental theoretical studies is presented. We found an intramolecular 1,3-hydrogen transfer during the formation of **L^3** and **L^4**, which in the case of the latter plays an important role in the 1,5-dipolar cyclization of **L^5**. The spectral changes that originate from an intramolecular charge transfer (ICT) in the form of a $\pi_{py} \rightarrow \pi^*_{napy}$ transition can be tuned through acid/base-controlled switching for **L^1**−**L^3**. A photoinduced isomerization for **L^1**−**L^3**, **1**, and **2** having flexible structures was observed under 365 nm light irradiation. Quantum chemical calculations revealed that the dinuclear complexes with structural asymmetry exhibit different metal-to-ligand charge-transfer transitions.

Introduction

A number of 1,8-naphthyridine derivatives have been synthesized over the past few decades because of their biocompatibility[1] and their good fluorescence properties.[2] Studies concerned with naphthyridine rings have shown that the N atoms in these compounds can effectively bind with the nitrogenous bases of DNA through hydrogen bonding, which allows for potential applications of the 1,8-naphthyridyl derivatives in medical and biological fields.[3−5] Additional research effort on luminescent naphthyridine derivatives and their Zn(II), Cu(I) complexes has focused on emissive $\pi\pi^*$ or metal-to-ligand charge-transfer (MLCT) excited states which can be tuned by hydrogen-bonding sites leading to intra- or intermolecular interactions.[6,7] The luminescent spectroscopic changes induced through hydrogen transfer and multiple hydrogen-bonding interactions have been used to produce luminescent sensors for biomedical applications.[8] Furthermore, Co(II),[9] Ru(II), and Ir(III)

*To whom correspondence should be addressed. E-mail: fuwf@mail.ipc.ac.cn.

(1) (a) Eldrup, A. B.; Christensen, C.; Haaima, G.; Nielsen, P. E. *J. Am. Chem. Soc.* **2002,** *124,* 3254–3262. (b) Nakatani, K.; Horie, S.; Saito, I. *J. Am. Chem. Soc.* **2003,** *125,* 8972–8973.

(2) (a) Fang, J. M.; Selvi, S.; Liao, J. H.; Slanina, Z.; Chen, C. T.; Chou, P. T. *J. Am. Chem. Soc.* **2004,** *126,* 3559–3566. (b) Hikishima, S.; Minakawa, N. *Angew. Chem., Int. Ed.* **2005,** *44,* 596–598. (c) Katz, J. L.; Geller, B. J.; Foster, P. D. *Chem. Commun.* **2007,** 1026–1028.

(3) (a) He, C.; Lippard, S. J. *J. Am. Chem. Soc.* **2000,** *122,* 184–185. (b) Smith, E. A.; Kyo, M.; Kumasawa, H.; Nakatani, K.; Saito, I.; Corn, R. M. *J. Am. Chem. Soc.* **2002,** *124,* 6810–6811.

(4) (a) Kobori, A.; Nakatani, K. *Bioorg. Med. Chem.* **2008,** *16,* 10338–10344. (b) Dohno, C.; Uno, S. N.; Sakai, S.; Oku, M.; Nakatani, K. *Bioorg. Med. Chem.* **2009,** *17,* 2536–2543.

(5) (a) Eldrup, A. B.; Nielsen, B. B.; Haaima, G.; Rasmussen, H.; Kastrup, J. S.; Christensen, C.; Nielsen, P. E. *Eur. J. Org. Chem.* **2001,** 1781–1790. (b) Peng, T.; Nakatani, K. *Angew. Chem., Int. Ed.* **2005,** *44,* 7280–7283. (c) Minakawa, N.; Ogata, S.; Takahashi, M.; Matsuda, A. *J. Am. Chem. Soc.* **2009,** *131,* 1644–1645.

(6) (a) He, C.; DuBois, J. L.; Hedman, B.; Hodgson, K. O.; Lippard, S. J. *Angew. Chem., Int. Ed.* **2001,** *40,* 1484–1487. (b) Takei, F.; Suda, H.; Hagihara, M.; Zhang, J.; Kobori, A.; Nakatani, K. *Chem.—Eur. J.* **2007,** *13,* 4452–4457.

(7) (a) He, C.; Lippard, S. J. *Inorg. Chem.* **2000,** *39,* 5225–5231. (b) Araki, H.; Tsuge, K.; Sasaki, Y.; Ishizaka, S.; Kitamura, N. *Inorg. Chem.* **2007,** *46,* 10032–10034.

(8) (a) Dohno, C.; Uno, S. N.; Nakatani, K. *J. Am. Chem. Soc.* **2007,** *129,* 11898–11899. (b) de Greef, T. F. A.; Ligthart, G. B. W. L.; Lutz, M.; Spek, A. L.; Meijer, E. W.; Sijbesma, R. P.; Dohno, C.; Uno, S. N.; Nakatani, K. *J. Am. Chem. Soc.* **2008,** *130,* 5479–5486. (c) Kuykendall, D. W.; Anderson, C. A.; Zimmerman, S. C. *Org. Lett.* **2009,** *11,* 61–64.

Scheme 1
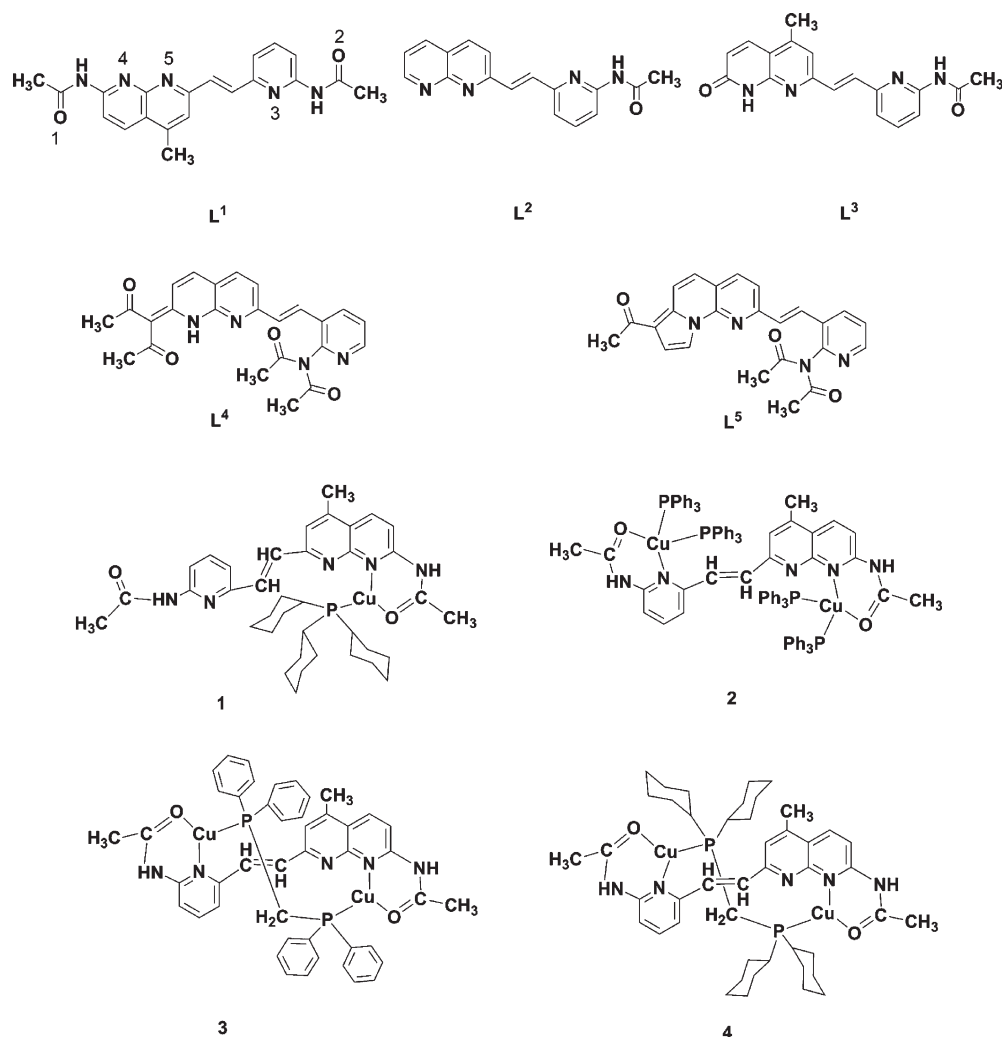
complexes containing the 1,8-naphthyridine derivatives have been synthesized, and their magnetic and catalytic properties have been investigated.[10] The 1,8-naphthyridyl compounds with flexible structures have not yet been exploited despite the large amount of reports on 1,8-naphthyridine derivatives and their complexes.[11,12] Previous study on luminescent copper(I) and platinum(II) complexes with a flexible naphthyridine-phosphine ligand demonstrated that this class of ligand exhibits various intriguing coordination modes and bonding properties.[13] A flexible ligand bis(7-methyl-1,8-naphthyridine-2-ylamino)methane with η^4-chelating and η^2-bridging modes has been synthesized and reported. Its Zn(II) and Cd(II) complexes display intense solution emissions. The fluorescence of the ligand bound to Cd(II) was found to be more pronounced than that with other cations, and this

property can thus be applied to Cd(II) ion recognition.[14] Recently, we conducted a two-electron reduction of azo-1,8-naphthyridine with anionic CH_3COO^- according to the Kolbe reaction.[15] Herein, we report on the synthesis and characterization of a series of new compounds $\mathbf{L^1}-\mathbf{L^5}$ in which a 1,8-naphthyridinyl segment and a pyridinyl group are connected by a vinyl bridge (Scheme 1). We also propose a mechanism for the synthesis of $\mathbf{L^5}$ and report on the synthesis of one mononuclear complex [CuL^1(PCy$_3$)](BF$_4$)$_2$ (**1**) and three dinuclear copper(I) complexes [Cu$_2$L^1(PPh$_3$)$_4$]-(BF$_4$)$_2$ (**2**), [Cu$_2$L^1(dppm)](BF$_4$)$_2$ (**3**), and [Cu$_2$(L^1)(dcpm)]-[BF$_4$]$_2$ (**4**). Time-dependent density functional theory (TD-DFT) calculations reveal some interesting photochemical and photophysical properties.

Experimental Section

General Comments. All the reactions were performed under a nitrogen atmosphere. Reagent grade solvents were dried by standard procedures and freshly distilled before use. The solvents used for spectroscopic measurements were HPLC grade. All other chemicals were obtained from commercial sources and

(9) Chien, C. H.; Chang, J. C.; Yeh, C. Y.; Lee, G. H.; Fang, J. M.; Peng, S. M. *Dalton Trans.* **2006**, 2106–2113.

(10) (a) Nakajima, H.; Tanaka, K. *Angew. Chem., Int. Ed.* **1999**, *38*, 362–363. (b) Zong, R.; Thummel, R. P. *J. Am. Chem. Soc.* **2005**, *127*, 12802–12803. (c) Sinha, A.; Wahidur Rahaman, S. M.; Sarkar, M.; Saha, B.; Daw, P.; Bera, J. K. *Inorg. Chem.* **2009**, *48*, 11114–11122.

(11) Bera, J. K.; Sadhukhan, N.; Majumdar, M. *Eur. J. Inorg. Chem.* **2009**, 4023–4038.

(12) Zuo, J. L.; Fu, W. F.; Che, C. M.; Cheung, K. K. *Eur. J. Inorg. Chem.* **2003**, 255–262.

(13) Zhang, J. F.; Fu, W. F.; Gan, X.; Chen, J. H. *Dalton Trans.* **2008**, 3093–3100.

(14) Zhang, H. M.; Fu, W. F.; Wang, J.; Gan, X.; Xu, Q. Q.; Chi, S. M. *Dalton Trans.* **2008**, 6817–6824.

(15) Fu, W. F.; Li, H. F. J.; Wang, D. H.; Zhou, L. J.; Li, L.; Gan, X.; Xu, Q. Q.; Song, H. B. *Chem. Commun.* **2009**, 5524–5526.

used without further purification. ^{1}H NMR spectra were recorded on a Bruker 400 or 500 MHz AVANCE II spectrometer at 298 K with chemical shifts (δ, ppm) relative to tetramethylsilane (Me$_4$Si) for ^{1}H. Electrospray ionization mass spectrometry (ESI-MS) data were obtained with an APEX II Model FT-ICR mass spectrograph. Matrix-assisted laser desorption/ionization-time of flight (MALDI-TOF) MS data were obtained on a Bruker Biflex III Model MALDI-TOF mass spectrograph. Elemental analyses were performed with an Elementar Vario EL (Germany) instrument. IR data were recorded on a Varian 3100 FTIR spectrometer. UV–vis spectra were obtained using a HITACHI U-3010 spectrophotometer. Corrected emission spectra of solutions and solids were obtained on a HITACHI F-4500 fluorescence spectrophotometer adapted to a right-angle configuration at room temperature. The emission lifetimes of solid or solution samples were determined using single photon counting on a FL920 Spectrometer (Edinburgh).

2-Amino-6-aldehydepyridine and 2-Amino-3-aldehydepyridine. The 2-amino-6-aldehydepyridine and 2-amino-3-aldehydepyridine were synthesized according to an improved method following reported procedures.[16,17]

2,4-Dimethyl-7-amino-1,8-naphthyridine.[18] 2,6-Diaminopyridine (10.90 g, 0.1 mol) and acetyl acetone (10.00 g, 0.1 mol) were mixed in 50 mL of acetic acid, and 1.5 mL of 96% sulfuric acid was added. The mixture was refluxed with stirring for 24 h under nitrogen atmosphere. The resulting solution was then cooled to room temperature, after which 150 mL of sodium hydroxide (6.67 M) solution was added slowly in ice bath. The precipitate was isolated by filtration, and washed with cool water (3 × 5 mL) and dried in vacuo. The crude product was recrystallized from ethanol by slow evaporation to give a pale yellow solid. Yield: 5.48 g (32%); m.p.: 220–221 °C; ^{1}H NMR (400 MHz, CDCl$_3$): δ = 2.52 (s, 3H; CH$_3$), 2.57 (s, 3H; CH$_3$), 6.67 (d, J = 9.7 Hz, 1H; Naph-H), 6.89 (s, 1H; Naph-H), 7.90 (d, J = 9.7 Hz, 1H; Naph-H); MS (EI): m/z (%): 173 (M^+).

2-(2-Acetylamino-pyridine-6-ethylene)-4-methyl-7-acetylamino-1,8-naphthyridine (L^1). 2,4-Dimethyl-7-amino-1,8-naphthyridine (0.90 g, 5.2 mmol) and 2-amino-6-aldehydepyridine (0.61 g, 5.0 mmol) were mixed in 20 mL of acetic anhydride. The mixture was refluxed with stirring for 24 h under nitrogen atomsphere. The resulting solution was added in 100 mL of ice water while hot, and then filtered after stirring for 1 h. The crude product was purified by column chromatography over silica gel column using chloroform/ethyl acetate/ethanol (1/10/1) as eluent to give ligand L^1 in the form of a yellow solid. Yield: 0.867 g (48%); ^{1}H NMR (400 MHz, CDCl$_3$): δ = 2.26 (s, 3H; COCH$_3$), 2.29 (s, 3H; COCH$_3$), 2.71 (s, 3H; 4-Me of naphthyridyl ring), 7.20 (d, J = 7.4 Hz, 1H; Py-H), 7.38 (s, 1H; Naph-H), 7.72 (m, 2H; Naph-H, Py-H), 7.91(d, J = 15.56, 1H; Py-H), 8.07 (s, 1H; NH), 8.14(d, J = 5.6 Hz, 1H; Naph-H), 8.34 (d, J = 9 Hz, 1H; CH), 8.48 (d, J = 9 Hz, 1H; CH), 8.68 (br, 1H; NH); MS (EI): m/z (%): 361 (M^+); elemental analysis calcd (%) for C$_{20}$H$_{19}$N$_5$O$_2$ (361.4): C, 66.47; H, 5.30; N, 19.38; found: C, 66.61; H, 5.21; N, 19.46.

2-(2-Acetylamino-pyridine-6-ethylene)-1,8-naphthyridine (L^2). The pale yellow compound was prepared following the same procedure as L^1 except that 2-methyl-1,8-naphthyridine was used instead of 2,4-dimethyl-7-amino-1,8-naphthyridine. Yield: (42%); ^{1}H NMR (400 MHz, CDCl$_3$): δ = 2.26 (s, 3H; COCH$_3$), 7.23 (m, 1H; Naph-H), 7.46 (m, 1H; Py-H), 7.68 (d, J = 8.4 Hz, 1H; Py-H), 7.75 (t, J = 7.9 Hz, 1H; Naph-H), 7.85 (d, J = 15.6 Hz, 1H; CH), 7.98 (d, J = 15.6 Hz, 1H; CH), 8.08 (br, 1H; NH), 8.17 (m, 1H; Py-H), 8.19 (m, 1H; Naph-H), 8.20 (m, 1H; Naph-H), 9,13 (m, 1H; Py-H); MS (EI): m/z (%): 289 (M−H)$^+$;

elemental analysis calcd (%) for C$_{17}$H$_{14}$N$_4$O (290.3): C 70.33, H 4.86, N 19.30; found: C 70.52, H 5.02, N 19.38.

2-(2-Acetylamino-pyridinyl-6-ethylene)-4-methyl-7-hydroxyl-1,8-naphthyridine (L^3). The compound was synthesized in the same way as L^1, from 2-amino-6-aldehydepyridine (0.61 g, 5.0 mmol) and 2,4-dimethyl-7-hydroxyl-1,8-naphthyridine (0.87 g, 5.0 mmol) that was prepared by a previously developed method.[19] Yellow single crystals were obtained by diffusion of diethyl ether into a dichloromethane solution. Yield: 0.593 g (37%); ^{1}H NMR (400 MHz, CDCl$_3$): δ = 2.27 (s, 3H; COCH$_3$), 2.50 (s, 3H; 4-Me of naphthyridyl ring), 6.67 (d, J = 9.6 Hz, 1H; CH), 6.70 (s, 1H; Naph-H), 7.14 (d, J = 7.4 Hz, 1H; Naph-H), 7.42 (d, J = 15.5 Hz, 1H; Py-H), 7.70 (m, 2H; Naph-H, Py-H), 7.86 (d, J = 9.6 Hz, 1H; CH), 8.17(d, J = 7.7 Hz, 1H; Py-H), 9.00 (s, 1H; OH), 10.20 (s, 1H; NH); MS (EI): m/z (%): 319 (M−H)$^+$; elemental analysis calcd (%) for C$_{18}$H$_{16}$N$_4$O$_2$ (320.4): C 67.49, H 5.03, N 17.49; found: C 67.28, H 5.10, N 17.63.

2-(2-Diacetylamino-pyridinyl-3-ethylene)-7-diacetylamino-1,8-naphthyridine (L^4). 2,7-Dimethyl-1,8-naphthyridine (1.00 g, 6.3 mmol) was added to a solution of 2-amino-3-aldehydepyridine[20] (1.00 g, 8.2 mmol) in 20 mL of normal acetic anhydride, and then the mixture was heated at reflux for 10 h under nitrogen atmosphere. The resulting solution was concentrated. The crude product was purified by column chromatography over silica gel column using chloroform and then 10% ethyl acetate/petroleum ether as eluents to give a red solid. Red crystals suitable for X-ray diffraction were obtained by diffusion of diethyl ether into a dichloromethane solution.Yield: 0.25 g (9.2%); m.p.: 197−198 °C. ^{1}H NMR (500 MHz, CDCl$_3$): δ = 13.88 (s, 1H), 8.56 (d, J = 3.4 Hz, 1H), 8.15 (d, J = 7.2 Hz, 1H), 7.63 (d, J = 7.8 Hz, 1H), 7.54 (d, J = 15.9 Hz, 1H), 7.45 (dd, J = 4.7 Hz, J = 7.7 Hz, 1H), 7.32 (dd, J = 9.2 Hz, J = 14.0 Hz, 1H), 7.14 (m, 1H), 7.12 (m, 1H), 6.55 (d, J = 9.2 Hz, 1H), 5.36 (s, 1H), 2.36 (s, 6H), 2.19 (s, 3H); ^{13}C NMR (125 MHz, CDCl$_3$): δ = 195.4, 172.5, 155.2, 151.4, 150.8, 149.4, 148.7, 135.9, 135.4, 134.1, 132.6, 131.1, 126.9, 124.9, 123.6, 118.4, 117.3, 94.3, 29.3, 26.5; IR (KBr, ν_{max}/cm^{-1}): 1723, 1702, 1619; TOF MS (EI): m/z (%): 431 (M+H)$^+$; elemental analysis calcd (%) for C$_{24}$H$_{22}$N$_4$O$_4$ (430.5): C 66.97, H 5.15, N 13.02; found: C 66.57, H 5.45, N 12.67.

7-(2-Diacetylamino-pyridinyl-3-ethylene)-4′-acetyl-pyrrolo-[1′,5′-a]-1,8-naphthyridine (L^5). 2,7-Dimethyl-1,8-naphthyridine (2.00 g, 12.6 mmol) was added to a solution of 2-amino-3-aldehydepyridine (1.55 g, 12.7 mmol) in 30 mL of anhydrous acetic anhydride, and then the mixture was heated at reflux for 24 h under nitrogen atmosphere. The resulting solution was concentrated. The crude product was purified by column chromatography over silica gel column using 15% ethyl acetate/petroleum ether as eluent to afford a brown solid, which was recrystallized from CH$_2$Cl$_2$/diethyl ether to give a brown crystal. Yield: 0.55 g (10.6%); m.p.: 226−227 °C; ^{1}H NMR (500 MHz, CDCl$_3$): δ = 8.60 (m, 1H), 8.36 (d, J = 9.3 Hz, 1H), 8.28 (d, J = 3.0 Hz, 1H), 8.24 (d, J = 7.8 Hz, 1H), 8.03 (d, J = 8.0 Hz, 1H), 7.71 (d, J = 15.9 Hz, 1H), 7.49 (m, 1H), 7.45 (d, J = 8.0 Hz, 1H), 7.32 (d, J = 4.5 Hz, 1H), 7.30 (m, 1H), 7.19 (d, J = 3.1 Hz, 1H), 2.61 (s, 3H), 2.39 (s, 6H); ^{13}C NMR (125 MHz, CDCl$_3$): δ = 194.3, 172.5, 152.8, 150.9, 149.6, 143.0, 137.0, 135.4, 133.8, 132.3, 130.9, 126.5, 124.8, 122.5, 120.6, 120.3, 118.8, 117.8, 115.0, 113.6, 28.4, 26.5; IR (KBr, ν_{max}/cm^{-1}): 1721, 1707, 1643; TOF MS (EI): m/z (%): 412 (M^+); elemental analysis calcd (%) for C$_{24}$H$_{20}$N$_4$O$_3$ (412.4): C 69.89, H 4.89, N 13.58; found: C 69.53, H 5.12, N 13.24.

[Cu(L^1)(PCy$_3$)]BF$_4$ (1). Ligand L^1 (0.072 g, 0.2 mmol) and Cu(CH$_3$CN)$_4$BF$_4$ (0.126 g, 0.4 mmol) were mixed with stirring in dichloromethane (25 mL) under a nitrogen atmosphere, and the reaction was accompanied by production of a yellow precipitate. After stirring for 3 h at room temperature, upon

(16) He, C.; Lippard, S. *Tetrahedron* **2000**, *56*, 8245–8252.

(17) Liang, F. S.; Xie, Z. Y.; Wang, L. X. *Tetrahedron Lett.* **2002**, *43*, 3427–3430.

(18) Henry, R. A.; Hammond, P. R. *J. Heterocyclic Chem.* **1977**, *14*, 1109–1114.

(19) Brown, E. V. *J. Org. Chem.* **1965**, *30*, 1607–1610.

(20) Majewicz, T. G.; Caluwe, P. *J. Org. Chem.* **1974**, *39*, 720–721.

Table 1. Selected Crystallographic and Data Collection Parameters for L^3–L^5 and **1**–**4**

	L^3	L^4	L^5	1	2	3	4
formula	$C_{19}H_{22}N_4O_4$	$C_{24}H_{22}N_4O_4$	$C_{24}H_{20}N_4O_3$	$C_{38}H_{52}BCuF_4N_5O_2P$	$C_{190.5}H_{171.5}B_4Cu_4F_{16}Cl_{8.5}N_{10}O_{4.5}P_8$	$C_{47}H_{45}B_2Cl_4Cu_2F_8N_5O_2P_2$	$C_{46}H_{64}B_2Cl_2Cu_2F_8N_5O_2P_2$
formula weight	370.41	430.46	412.44	792.17	3823.36	1216.32	1152.56
T [K]	293(2)	298(2)	294(2)	293(2)	294(2)	293(2)	293(2)
crystal size [mm]	0.43 × 0.35 × 0.31	0.56 × 0.42 × 0.30	0.22 × 0.16 × 0.10	0.18 × 0.16 × 0.08	0.26 × 0.24 × 0.20	0.28 × 0.22 × 0.16	0.16 × 0.16 × 0.14
crystal system	monoclinic	triclinic	monoclinic	triclinic	triclinic	triclinic	triclinic
space group	P2(1)/n	P$\bar{1}$	P2(1)/c	P$\bar{1}$	P$\bar{1}$	P$\bar{1}$	P$\bar{1}$
a [Å]	7.109(2)	8.1747(9)	11.599(2)	10.908(3)	18.606(2)	12.133(2)	12.433(4)
b [Å]	19.665(5)	10.968(2)	22.941(4)	12.499(3)	20.521(2)	14.930(3)	13.295(4)
c [Å]	13.658(4)	13.163(2)	7.953(1)	15.228(4)	25.548(3)	14.932(3)	19.041(6)
α [deg]	90.00	72.119(2)	90.00	74.782(4)	87.966(2)	80.844(3)	98.253(6)
β [deg]	103.784(6)	88.134(3)	105.636(7)	79.373(5)	85.734(2)	88.464(3)	106.798(6)
γ [deg]	90.00	73.414(2)	90.00	77.383(5)	88.467(2)	85.300(3)	100.550(6)
V [Å^3]	1854.4(9)	1074.5(3)	2037.8(6)	1937.1(9)	9718.7(19)	2661.2(8)	2896.9(17)
Z	4	2	4	2	2	2	2
ρ_{calcd} [g cm^{-3}]	1.327	1.330	1.344	1.358	1.307	1.518	1.321
$2\theta_{max}$ [deg]	50.00	50.02	50.34	52.76	50.00	52.82	50
μ [mm^{-1}]	0.095	0.093	0.091	0.664	0.684	1.131	0.945
reflections collected/unique	9523/3261	5595/3732	11561/4253	11161/7821	49939/34021	15515/10785	14998/10132
parameters	254	298	283	509	2201	729	781
R_{int}	0.0465	0.0249	0.0329	0.0350	0.0348	0.0258	0.0345
goodness of fit	1.204	1.015	1.013	1.008	1.009	1.002	1.019
$R1$, $wR2$[all data]	0.1104, 0.2001	0.0925, 0.1462	0.0892, 0.1216	0.1162, 0.1290	0.1668, 0.3249	0.1189, 0.1587	0.1364/0.2382
$R1$, $wR2$[$I > 2\sigma(I)$]	0.0632, 0.1712	0.0477, 0.1150	0.0427, 0.0987	0.0515, 0.0987	0.0876, 0.2537	0.0574, 0.1444	0.0691/0.1939
residual electron density [e Å^{-3}]	−0.208/0.320	−0.196/0.181	−0.203/0.155	−0.435/0.401	−0.922/1.233	−0.513/0.791	−0.383/0.901

$R1 = \sum ||F_o| - |F_c||/\sum |F_o|$. $wR_2 = \{\sum w(F_o{}^2 - F_c{}^2)^2/\sum w(F_o{}^2)^2\}^{1/2}$.

addition of PCy_3 (0.234 g, 0.8 mmol) the yellow suspension dissolved gradually, the resulting solution was stirred for another 2 h and then filtered. The filtration was concentrated in vacuum, and the crude product was recrystallized from CH_2Cl_2/diethyl ether to give a yellow solid. Yellow crystals were obtained by diffusion of diethyl ether into a dichloromethane solution. Yield: (39%). The yellow crystalline solid was characterized by ^{1}H NMR, elemental analysis, and X-ray crystallography. ^{1}H NMR (400 MHz, CDCl$_3$): $\delta = 1.20-1.88$ (m, 33H; Cy), 2.16 (s, 3H; CH$_3$), 2.20 (s, 3H; CH$_3$), 2.23 (s, 3H; CH$_3$), 7.10 (d, 1H; Py-H), 7.30 (s, 1H; Naph-H), 7.50–7.65 (m, 2H; Naph-H), 7.83–7.98 (m, 2H; Naph-H, Py-H), 8.03 (s, 1H; NH), 8.16 (d, 1H; CH), 8.32 (d, 1H; CH); elemental analysis calcd (%) for $C_{38}H_{52}BCuF_4N_5O_2P$ (1792.18): C 57.61, H 6.62, N 8.84; found: C 57.93, H 6.79, N 8.78.

[Cu$_2$(L^1)(PPh$_3$)$_4$](BF$_4$)$_2$ (2). Complex **2** was obtained by reacting Cu(CH$_3$CN)$_4$BF$_4$, **L^1** and PPh$_3$ in a stoichiometric ratio of 2:1:4 in dichloromethane and via the same procedure as for **1**. Yield: (58%). The crystalline solid was characterized by ^{1}H NMR, elemental analysis and X-ray crystallography. ^{1}H NMR (400 MHz, CDCl$_3$): $\delta = 2.08$ (s, 3H; CH$_3$), 2.11 (s, 3H; CH$_3$), 2.19 (s, 3H; CH$_3$), 6.70 (d, 1H; Py-H), 7.08 (t, 26H; Ph-H), 7.15 (d, 24H; Ph-H), 7.25 (m, 13H; Naph-H, Ph-H), 7.45 (t, 1H; Py-H), 7.57 (d, 2H; CH), 7.66 (br, 2H; NH), 7.76 (d, 1H; Py-H); elemental analysis calcd (%) for $C_{92}H_{79}B_2Cu_2F_8N_5O_2P_4$ (powders, 1711.24): C 64.57, H 4.65, N 4.09; found: C 64.85, H 4.92, N 4.37.

[Cu$_2$(L^1)(dppm)](BF$_4$)$_2$ (3). A mixture of **L^1** (0.072 g, 0.2 mmol), Cu(CH$_3$CN)$_4$BF$_4$ (0.126 g, 0.4 mmol) in dichloromethane (30 mL) was stirred for 4 h under a nitrogen atmosphere at room temperature, resulting in a yellow precipitate. After adding dppm (0.154 g, 0.4 mmol) the precipitate was dissolved slowly to give a yellow solution. The solvent was removed in vacuo leaving an orange solid. Orange crystals of **3** suitable for an X-ray crystallograph structure determination were obtained by vapor diffusion of diethyl ether into solution of crude product in dichloromethane. Yield: (0.163 g, 78%). The crystalline solid was characterized by ^{1}H NMR, elemental analysis, and X-ray crystallography. ^{1}H NMR (400 MHz

DMSO-d$_6$): $\delta = 2.05$ (s, 3H; CH$_3$), 2.09 (s, 3H; CH$_3$), 2.13 (s, 2H; CH$_2$), 2.70 (s, 3H; CH$_3$), 6.59 (t, 2H; Ph-H), 6.67 (d, 2H; Ph-H), 6.84 (t, 2H; Ph-H), 6.90 (t, 2H; Ph-H), 6.96 (t, 2H; Ph-H), 7.03 (t, 2H; Ph-H), 7.10 (t, 2H; Ph-H), 7.18–7.43 (m, 12H; Ar–H), 7.52 (t, 1H; Py-H), 7.65 (br, 2H; NH), 7.70 (d, 1H; Py-H); elemental analysis calcd (%) for $C_{45}H_{41}B_2Cu_2F_8N_5O_2P_2$ (1046.49): C 51.65, H 3.95, N 6.69; found: C 51.85, H 4.22, N 4.37.

**[Cu$_2$(L^1)(dcpm)](BF$_4$)$_2$ (4).** The orange crystals of complex **4** were obtained following the same procedure as **3** except that dcpm was used, and Cu(CH$_3$CN)$_4$BF$_4$, **L^1**, and bis(dicyclohexyl-phosphino)methane (dcpm) are in a stoichiometric ratio of 2:1:1. Yield: (62%). The yellow crystalline solid was characterized by ^{1}H NMR, elemental analysis, and X-ray crystallography. ^{1}H NMR (400 MHz, CDCl$_3$): $\delta = 1.18-2.02$ (m, 44H; dcpm-H), 2.12–2.21 (m, 9H; CH$_3$), 3.02 (s, 2H; CH$_2$), 7.06 (d, 1H; Py-H), 7.12 (s, 1H; Naph-H), 7.41 (t, 1H; Py-H), 7.58 (d, 1H; Naph-H), 7.68 (d, 1H; Py-H), 8.04 (d, 1H; Naph-H), 8.14 (d, 1H; CH), 8.20 (d, 1H; CH), elemental analysis calcd (%) for $C_{45}H_{65}B_2Cu_2F_8N_5O_2P_2$ (1070.68): C, 50.48, H 6.12, N 6.52; found: C 50.26, H 6.04, N 6.46.

X-ray Crystallography. Crystals suitable for X-ray structure determination were obtained by the diethyl ether diffusion method. X-ray data were collected on a Bruker SMART X-ray diffractometer using a graphite monochromator with Mo−Kα radiation (λ = 0.071073 nm) at room temperature. A summary of the crystallographic parameters and data is given in Table 1. The structures were solved by direct methods (SHELXL 97) and refined by full-matrix least-squares methods on all F^2 data.[21,22] Metal atoms in each complex were located from the E-maps and other non-hydrogen atoms were located in successive difference Fourier syntheses. The hydrogen atoms of the ligands were generated theoretically onto the specific atoms and refined isotropically with fixed thermal factors.

(21) Sheldrick, G. M. *SHELXS 97, Program for the Solution of Crystal Structure*; University of Göttingen: Göttingen, Germany, 1997.
(22) Sheldrick, G. M. *SHELXL97, Program for the Refinement of Crystal Structures*; University of Göttingen: Göttingen, Germany, Germany, 1997.

Scheme 2
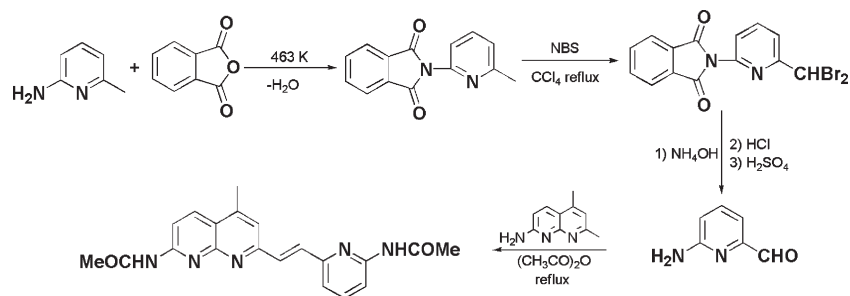
TD-DFT Calculations. All optimizations were carried out with the Gaussian 03 program package[23] using the 6-311+G* basis set,[24,25] with the hybrid density functional theory (B3LYP) employed.[26,27] Time-dependent density functional theory at the TD-DFT(B3LYP/6-311+G*) level were also carried out with the Gaussian 03 program to predict and verify the absorption spectra of various species.

Results and Discussion

Synthesis and X-ray Characterization. Yields of the 1,8-naphthyridine derivatives used as starting materials can be improved by increasing the solution alkalinity. L^1-L^3 were synthesized by refluxing the corresponding 1,8-naphthyridine derivatives and 2-amino-6-aldehydepyridine in normal or anhydrous acetic anhydride (Scheme 2). The condensed compounds were isolated in yields of 19−36%, and they are freely soluble in organic solvents such as CH_2Cl_2, CH_3CN, and MeOH.

The reaction of 2,7-dimethyl-1,8-naphthyridine with 2-amino-3-aldehydepyridine in normal acetic anhydride under reflux yields an unexpected compound L^4 containing a β-diketone group. In anhydrous acetic anhydride, the subsequent reaction of L^4 leads to the indolizine derivatives of 1,8-naphthyridine (L^5). A structural investigation of L^4 indicates that intramolecular 1,3-hydrogen transfer occurs during the formation of the compound, and this plays an important role during the production of L^5. Several methods of synthesizing indolizine derivatives of pyridine have been reported and reviewed in the literature.[28] Our group was the first to report on the synthesis

Scheme 3
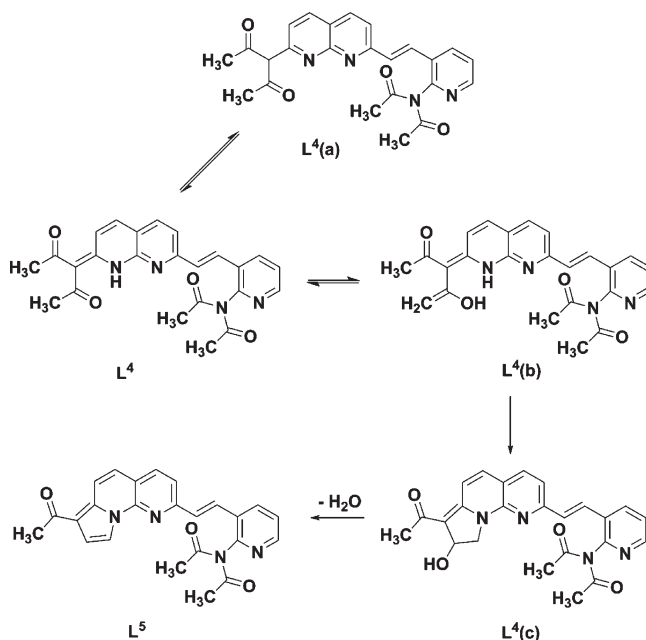
of pyrrolo[1′,5′-a]-1,8-naphthyridinederivatives.[29,30] Generally, a five-membered ring moiety is formed in the indolizine framework through intramolecular or intermolecular condensation by 1,3-dipolar cycloaddition[31,32] or 1,5-dipolar cyclization[33,34] To investigate the mechanism for the formation of L^5, we chose L^4 as the starting reactant, anhydrous acetic anhydride as the solvent, and L^5 was obtained in 60% yield. The suggested mechanism is shown in Scheme 3. L^4 is in a tautomeric form of the intermediates, L^4(a) or L^4(b), and undergoes ring closure to L^4(c) followed by a dehydration leading to L^5. A similar mechanism has previously been proposed by Chichibabin and Stepanow,[35] but no structural analysis was reported.

L^1 reacts with $[Cu(CH_3CN)_4]BF_4$ and PCy_3, PPh_3, dppm, or dcpm to afford the mono- or dinuclear

(23) Frisch, M. J.; Trucks, G. W.; Schlegel, H. B.; Scuseria, G. E.; Robb, M. A.; Cheeseman, J. R.; Montgomery, J. A.; Vreven, Jr., T.; Kudin, K. N.; Burant, J. C.; Millam, J. M.; Iyengar, S. S.; Tomasi, J.; Barone, V.; Mennucci, B.; Cossi, M.; Scalmani, G.; Rega, N.; Petersson, G. A.; Nakatsuji, H.; Hada, M.; Ehara, M.; Toyota, K.; Fukuda, R.; Hasegawa, J.; Ishida, M.; Nakajima, T.; Honda, Y.; Kitao, O.; Nakai, H.; Klene, M.; Li, X.; Knox, J. E.; Hratchian, H. P.; Cross, J. B.; Adamo, C.; Jaramillo, J.; Gomperts, R.; Stratmann, R. E.; Yazyev, O.; Austin, A. J.; Cammi, R.; Pomelli, C.; Ochterski, J. W.; Ayala, P. Y.; Morokuma, K.; Voth, G. A.; Salvador, P.; Dannenberg, J. J.; Zakrzewski, V. G.; Dapprich, S.; Daniels, A. D.; Strain, M. C.; Farkas, O.; Malick, D. K.; Rabuck, A. D.; Raghavachari, K.; Foresman, J. B.; Ortiz, J. V.; Cui, Q.; Baboul, A. G.; Clifford, S.; Cioslowski, J.; Stefanov, B. B.; Liu, G.; Liashenko, A.; Piskorz, P.; Komaromi, I.; Martin, R. L.; Fox, D. J.; Keith, T.; Al-Laham, M. A.; Peng, C. Y.; Nanayakkara, A.; Challacombe, M.; Gill, P. M. W.; Johnson, B.; Chen, W.; Wong, M. W.; Gonzalez, C.; Pople, J. A. *Gaussian 03*, Revision C.02; Gaussian, Inc.: Wallingford, CT, 2004.
(24) Krishnan, R.; Binkley, J. S.; Seeger, R.; Pople, J. A. *J. Chem. Phys.* **1980**, *72*, 650–654.
(25) Clark, T.; Chandrasekhar, J.; Spitznagel, G. W.; Schleyer, P. V. R. *J. Comput. Chem.* **1983**, *4*, 294–301.
(26) Becke, A. D. *J. Chem. Phys.* **1993**, *98*, 5648–5652.
(27) Lee, C.; Yang, W.; Parr, R. G. *Phys. Rev. B* **1988**, *37*, 785–789.
(28) Borrows, E. T.; Holland, D. O. *Chem. Rev.* **1948**, *42*, 611–643.

(29) Zhao, X. J.; Chen, Y.; Fu, W. F.; Zhang, J. B. *Synth. Commun.* **2007**, *37*, 2145–2152.
(30) Gueiffier, A.; Blache, Y.; Viols, H.; Chapat, J. P.; Dauphin, G. *J. Heterocyclic Chem.* **1992**, *29*, 691–697.
(31) Scholtz, M. *Ber. Dtsch. Chem. Ges.* **1912**, *45*, 734–746.
(32) Kaloko, J., Jr.; Hayford, A. *Org. Lett.* **2005**, *7*, 4305–4308.
(33) Kakehi, A.; Suga, H.; Kako, T.; Fujii, T.; Tanaka, N.; Kobayashi, T. *Chem. Pharm. Bull.* **2003**, *51*, 1246–1252.
(34) Østby, O. B.; Dalhus, B.; Gundersen, L. L.; Rise, F.; Bast, A.; Haenen, G. R. M. M. *Eur. J. Org. Chem.* **2000**, 3763–3770.
(35) Tschitschibabin, A. E.; Stepanow, F. N. *Ber. Dtsch. Chem. Ges.* **1929**, *62*, 1068–1075.

Table 2. Selected Bond Lengths [Å] and Angles [deg] of L^3–L^5 and 1–4

	L^3				**L^4**		
C(1)−O(1)	1.236(3)	C(16)−N(4)−C(17)	130.3(3)	C(2)−C(14)	1.463(3)	C(2)−C(14)−C(15)	125.4(2)
C(7)−C(10)	1.461(4)	C(7)−C(10)−C(11)	126.0(3)	C(14)−C(15)	1.326(3)	C(9)−C(10)−O(1)	121.7(2)
C(10)−C(11)	1.327(4)	N(4)−C(17)−O(2)	121.9(3)	C(8)−C(9)	1.407(3)	C(16)−N(4)−C(23)	119.2(2)

	L^5		
N(2)−C(9)	1.382(2)	C(1)−C(14)−C(15)	125.3(2)
C(6)−C(11)	1.395(3)	C(6)−C(11)−C(10)	106.2(2)
C(9)−C(10)	1.359(3)	C(9)−N(2)−C(5)	127.8(2)
C(10)−C(11)	1.420(3)	C(6)−N(2)−C(9)	109.2(2)
C(14)−C(15)	1.325(3)	C(9)−C(10)−C(11)	109.4(2)

	1				**2**		
Cu(1)−N(1)	1.984(3)	N(2)−Cu(1)−O(1)	84.4(1)	Cu(2)−N(4)	2.130(6)	N(2)−Cu(1)−O(1)	84.3(2)
Cu(1)−O(1)	2.159(3)	N(1)−Cu(1)−P(1)	159.3(1)	Cu(2)−O(2)	2.117(6)	N(2)−Cu(1)−P(1)	118.1(2)
Cu(1)−P(1)	2.175(1)	P(1)−Cu(1)−O(1)	112.6(1)	Cu(2)−P(3)	2.295(2)	P(1)−Cu(1)−P(2)	126.74(9)

	3				**4**		
Cu(1)−N(2)	1.984(6)	N(2)−Cu(1)−O(1)	86.8(2)	Cu(2)−N(4)	1.981(6)	N(4)−Cu(2)−O(2)	88.7(7)
Cu(1)−O(1)	2.134(4)	N(2)−Cu(1)−P(1)	170.6(1)	Cu(2)−O(2)	2.07(2)	N(4)−Cu(2)−P(2)	155.1(2)
Cu(1)−P(1)	2.169(1)	P(1)−Cu(1)−O(1)	102.6(1)	Cu(2)−P(2)	2.164(2)	P(2)−Cu(2)−O(2)	116.2(7)
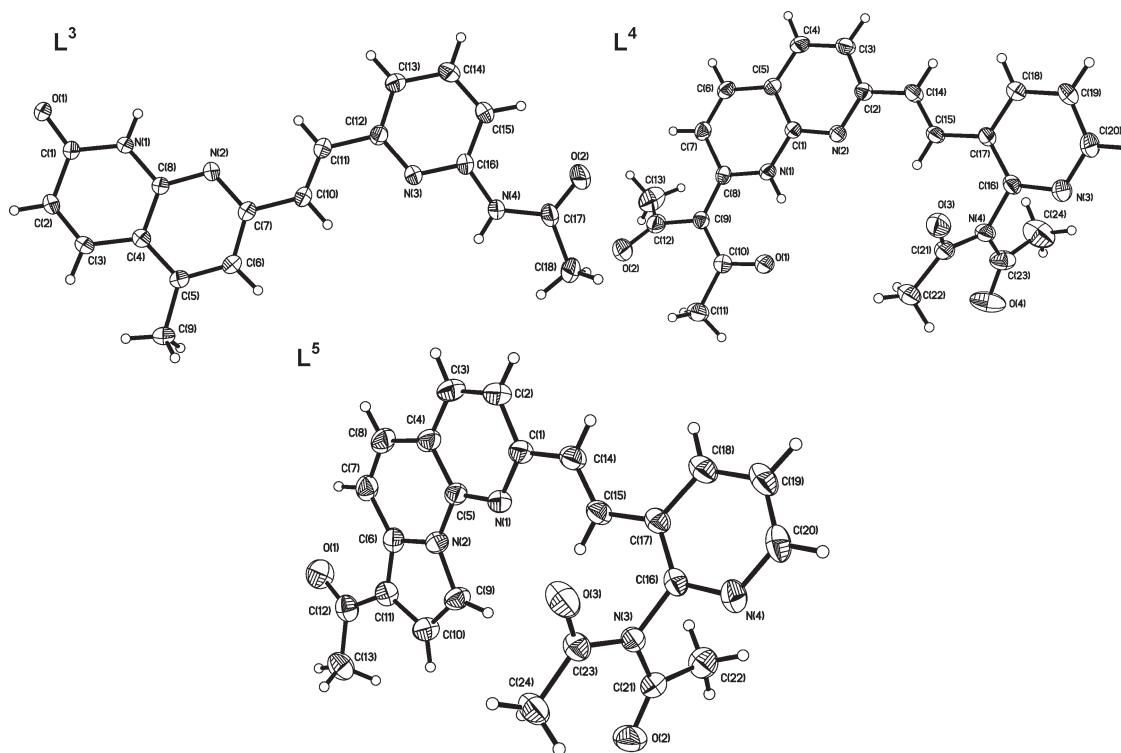
Figure 1. Perspective views of with labeling scheme for L^3–L^5. The thermal ellipsoids are at 30% probability.

complexes [Cu(L^1)PCy_3]BF_4 (**1**), [Cu_2(L^1)(PPh_3)_4](BF_4)_2 (**2**), [Cu_2(L^1)(dppm)](BF_4)_2 (**3**), and [Cu_2(L^1)(dcpm)]-(BF_4)_2 (**4**). Crystals of L^3−L^5 and **1**−**4** suitable for X-ray structural analysis were obtained by diethyl ether diffusion, and their structures were determined by X-ray diffraction analysis. The crystal data and details on data collection and refinement are summarized in Table 1. Selected bond lengths and angles are given in Table 2. The groups around the C=C double bond adopt a *trans*-configuration in the compounds. A structural investigation showed that the hydrogen atom on the hydroxyl of L^3 transfers to an adjacent naphthyridine-N atom leading to a keto configuration. A perspective view with a labeling

scheme is shown in Figure 1. The molecular naphthyridine and pyridine rings in L^3 are almost coplanar, and the two molecules in the unit cell in parallel planes are oriented head to tail. A π−π interaction with an average interplanar separation of 3.38 Å was observed in the crystal lattice. In the crystal structure of L^4, two methyl hydrogens at the 2-position of the naphthyridine moiety are substituted by acetyl groups, and a β-diketone is generated, which is accompanied by one hydrogen atom transfer to an adjacent naphthyridine-N atom and the −NH_2 forms a diacetylamino group. The hydrogen transfer results in the formation of a six-membered ring, N1−C8−C9−C10-O1···H1, with an
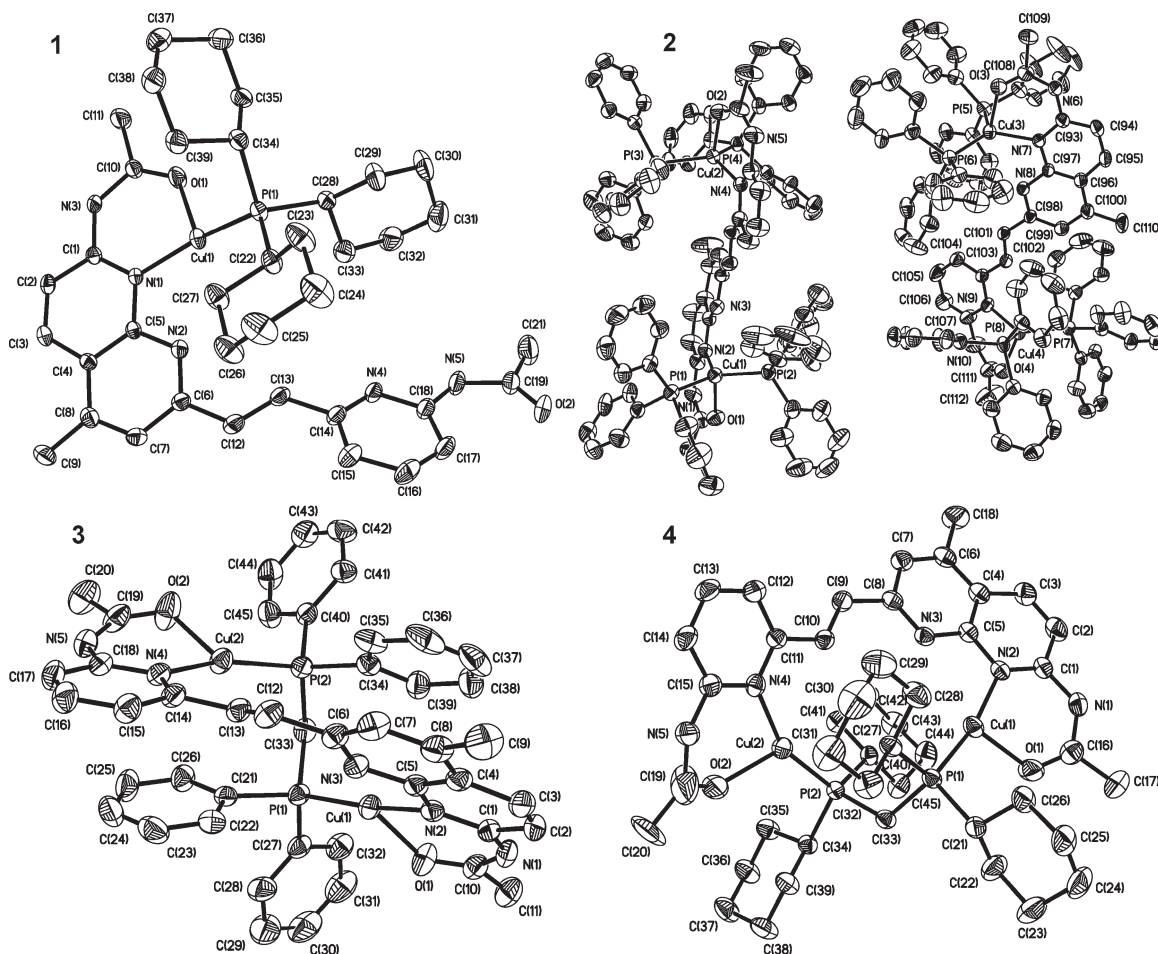
Figure 2. Perspective views with labeling scheme for **1**−**4**. The thermal ellipsoids are at 30% probability. All hydrogen atoms and solvent molecules have been omitted for clarity.

intramolecular hydrogen-bond length of 1.84 Å, and the distances of C(12)−O(2) and C(10)−O(1) are 1.233 and 1.251 Å, respectively (Figure 1). A perspective view of $\mathbf{L^5}$ is shown in Figure 1. In accordance with its aromaticity, the pyrrolo[1′,5′-*a*]-1,8-naphthyridine moiety in the molecule has a planar geometry, and all bond lengths and angles have values expected for aromatic compounds.

Complexes **1**−**4** exhibit different coordination modes depending on the nature of the phosphine ligands used. Their Oak Ridge thermal ellipsoid plot (ORTEP) diagrams along with the atom-numbering scheme are shown in Figure 2. When a mixture of $\mathbf{L^1}$, [Cu(CH$_3$CN)$_4$]BF$_4$, and the bulky ligand PCy$_3$ (1:2:4 molar ratio) in dichloromethane was stirred at room temperature, complex **1** was obtained as a mononuclear complex leaving a free acetylamino-pyridine moiety. The complex features T-shaped CuNPO geometry around the Cu atom, and the bond angles vary from 84.39 to 159.30° (Table 2). Compared with the copper(I) to naphthyridine-N bond length Cu(1)−N(1) of 1.984 Å, the Cu(1)···N(2) interaction distance is 2.748 Å (Figure 2). In contrast, the coordination geometry of Cu in the binuclear complex **2** is best described as a distorted tetrahedron with each copper(I) center coordinated to a naphthyridine- or pyridine-nitrogen atom, an acetyl oxygen atom as well as two PPh$_3$ ligands (Figure 2). The average Cu−N, Cu−O, and Cu−P distances are 2.099, 2.186, and 2.269 Å, respectively.

The bond angles at the copper atom vary from 82.8 to 126.74°. The crystal structures of **3** and **4** show that ligand $\mathbf{L^1}$ bridges two Cu(I) metal centers through the acetylamino-naphthyridine and -pyridine moieties. Addition of the bridging ligands, dppm, or dcpm generates a bimetallic 13-membered ring. The steric effect of both dppm and dcpm can be seen clearly by comparing the non-bonding Cu(I)···Cu(I) intra-separation with the former being 4.835 and latter 5.110 Å (Figure 2). Each copper atom has a slightly distorted planar trigonal geometry with bond angles at the copper atoms varying from 85.8 to 170.63°.
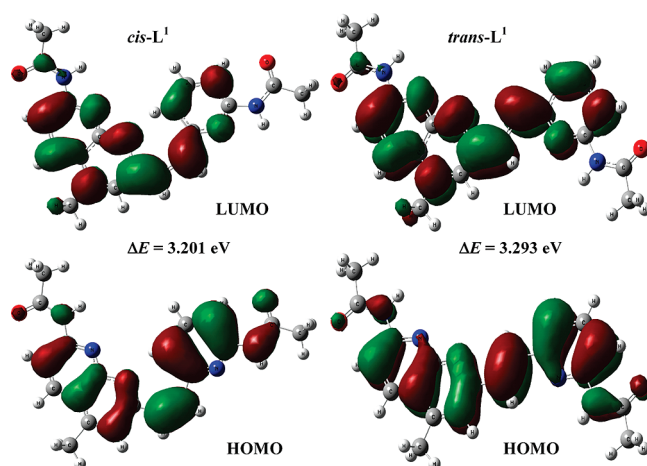
Spectroscopic Properties of $\mathbf{L^1}$−$\mathbf{L^5}$ and 1−4. The UV−vis absorption spectra of $\mathbf{L^1}$−$\mathbf{L^3}$ exhibit an intense transition at λ_{max} values ranging from 360 to 390 nm. In comparison, the absorptions centered at <390 nm for complexes **1**−**4** are similar to that of the ligand $\mathbf{L^1}$ but have tails extending from 400 to about 500 nm (Table 3). On the basis of a TD-DFT calculation (Figures 3 and 4), the lower-energy absorption bands of $\mathbf{L^1}$−$\mathbf{L^3}$ are assigned to an ICT $\pi_{py} \rightarrow \pi^*_{napy}$ transition. As shown in Figure 3, the highest occupied molecular orbital (HOMO) and the lowest unoccupied molecular orbital (LUMO) for **1** are mainly localized on the Cu(I) center and the naphthyridine moiety, respectively. However, the calculated energy gap of 567 nm from the HOMO to the LUMO does not correlate with the observed absorption spectrum. TD-DFT calculation demonstrates that the oscillator strength

Table 3. Spectroscopic Data of L^1–L^3 and **1**, **3**, and **4**

compound	medium (T[K])	λ_{abs}[nm] (ε[dm^3 mol^{-1} cm^{-1}])	λ_{em}[nm]	ϕ_{em}
L^1	CH$_3$CN (298)	363 (25200), 372 (25100)	399	
	CH$_2$Cl$_2$ (298)	365 (25500)	399, 415 (sh)	
	CH$_3$OH (298)	360 (25700), 373 (25900)	407	0.86
	solid (298)		491	
L^2	CH$_3$CN (298)	358 (11500)	411	
	CH$_2$Cl$_2$ (298)	359 (16400)	406	
	CH$_3$OH (298)	359 (13500)	429	
	solid (298)		526	
L^3	CH$_3$CN (298)	372 (13700), 389 (10440)	424	
	CH$_2$Cl$_2$ (298)	375 (12600), 393 (9812)	427	
	CH$_3$OH (298)	370 (13800), 388 (11200)	422	
	solid (298)		466	
1	CH$_3$CN (298)	361 (25490), 374 (26500)	400	
	CH$_2$Cl$_2$(298)	376 (29800)	395, 415 (sh)	
	CH$_3$OH (298)	360 (28890), 374 (29700)	410	0.6
	solid (298)			
3	CH$_3$CN (298)	364 (25300), 373 (25400)	403	
	CH$_2$Cl$_2$(298)	377 (28100), 393 (27700)	394 (sh), 416	
	CH$_3$OH (298)	375 (27400), 430(sh) (6486)	410	0.018
	solid (298)		452, 514	
4	CH$_3$CN (298)	364 (24640), 373 (24970)	412	
	CH$_2$Cl$_2$(298)	378 (25080), 395 (23100)	430	
	CH$_3$OH (298)	376 (25800), 425(sh) (3120)	428	0.045
	solid (298)		469, 524	
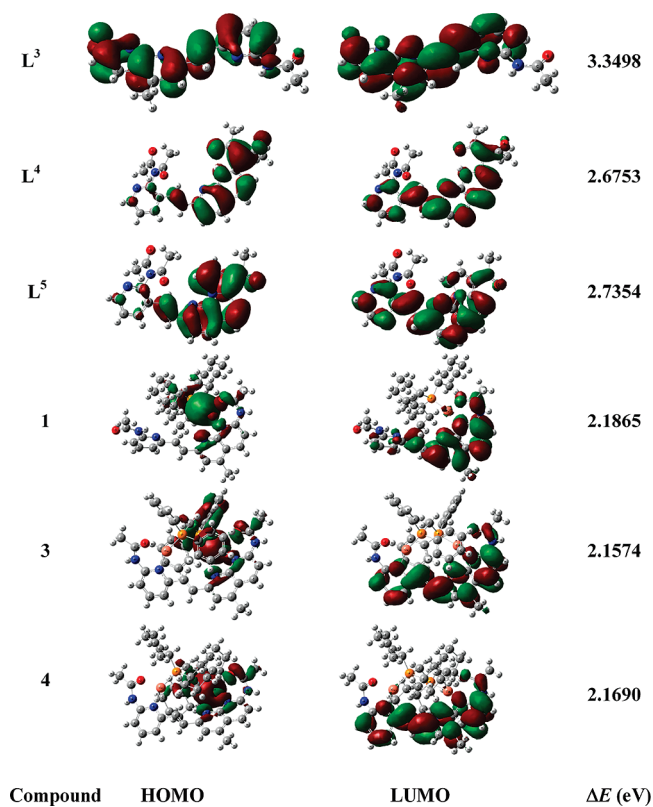
Figure 3. Plots of the relevant HOMO and LUMO for compounds L^3–L^5 and **1**–**4**.

Figure 4. Plots of the relevant HOMO and LUMO for compounds *cis*- and *trans*−L^1.

(*f*) values are 0.165 and 0.002 for the $\pi_{py} \rightarrow \pi^*_{napy}$ transition and the lower-energy gap, respectively. Thus, it is appropriate that the observed higher-energy absorption is assigned to a π_{py} electron to π^*_{napy} orbital transition (see the Supporting Information). The UV−vis absorption spectra of the dinuclear complexes **3** and **4** have a shoulder peak at about 430 nm. A quantum chemical calculation indicates that the asymmetrical complexes may undergo two different MLCT transitions originating

from the Cu-naphthyridine and the Cu-pyridine moieties. The excitation energy of the former ($d_{Cu} \rightarrow \pi^*_{napy}$) transition is lower than that of the latter and corresponds to an energy gap between HOMO and LUMO of 574.7 and 571.6 nm for **3** and **4**, the MLCT excitation energies from the $d_{Cu} \rightarrow \pi^*_{py}$ transition are 479 and 468 nm, respectively (see Supporting Information). We therefore attribute the observed lower-energy absorption to a $d_{Cu} \rightarrow \pi^*_{py}$ transition in nature. Compounds L^1−L^3 and complex **1** display an intense solution emission with a λ_{max} at 400−430 nm upon excitation at 360 nm. The fluorescence emissions originate from an intraligand excited state, and the photophysical data are listed in Table 3.

The absorption spectra of L^4 and L^5 in dichloromethane show intense low-energy absorption bands at 454 and 420 nm with large extinction coefficients of 15443 and 14960 mol^{-1} dm^3 cm^{-1}, respectively (Figure 5). The theoretical calculation reveals that the methyl-substituted naphthyridine unit is electron rich and acts as an electron donor in the molecules. The character of the LUMO is
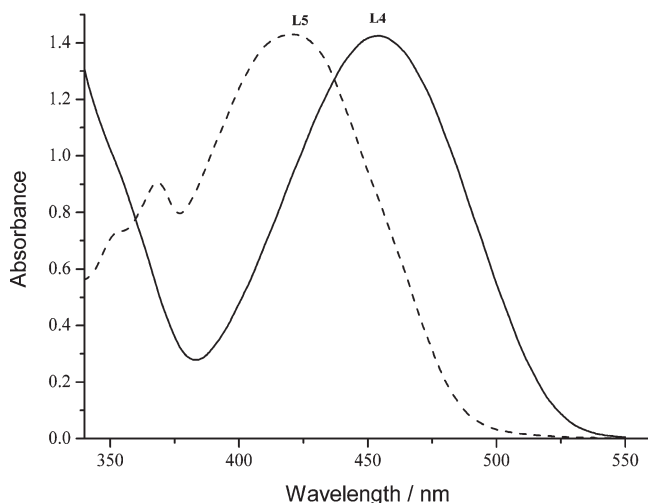
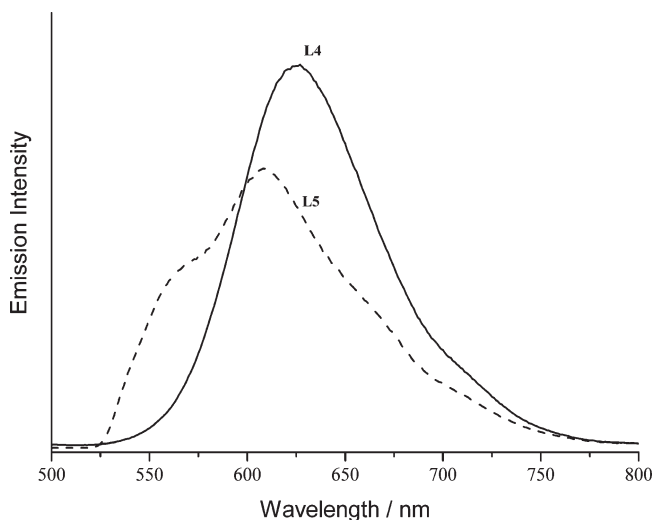**Figure 5.** UV−vis absorption spectra of the compounds L^4 and L^5 in dichloromethane.

Figure 6. Solid-state emission spectra of the compounds L^4 and L^5 upon excitation at 400 nm.

dominated by the pyridyl ring with a contribution from the naphthyridine moiety. The calculated energy gaps of L^4 and L^5 are consistent with the measured absorption energies and are 2.68 and 2.74 eV, (463 and 453 nm, Figure 3) respectively. The low-energy absorptions of L^4 and L^5 can be attributed to an ICT $\pi_{napy} \rightarrow \pi^*_{py}$ transition that is opposite to those of L^1-L^3.

Compound L^4 has an intense red luminescence with a λ_{max} at 626 nm in the solid state at room temperature. Compared to the emission of L^4, the solid powder of L^5 has a weaker photoluminescence with a λ_{max} at 607 nm (Figure 6). Upon excitation at 300 nm, compound L^5 displays an emission peak maximum at 520 nm in dichloromethane at room temperature, and the emission quantum yield is 0.58. Compound L^4 exhibits both high- and low-energy emissions with λ_{max} values at 393 and 593 nm while the overall emission quantum yield is 0.01.[36] The extended π-conjugated molecule with a rigid structure in L^5 leads to an enhancement of the emission intensity in solution.
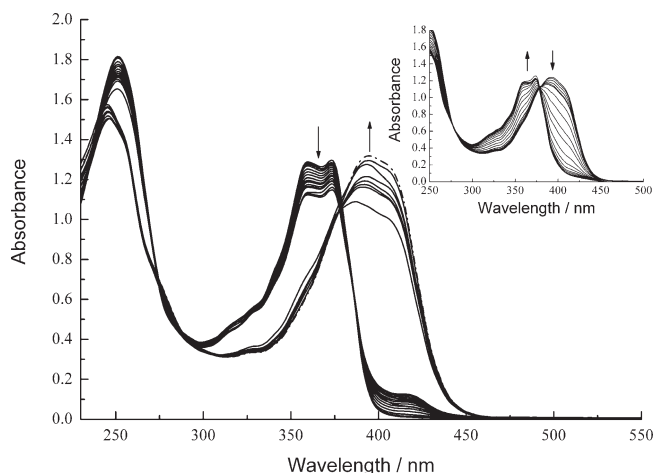
(36) Demas, J. N.; Crosby, G. A. *J. Phys. Chem.* **1971**, *75*, 991–1024.

Figure 7. Changes in the absorption spectra of L^1 (5.0×10^{-5} mol dm^{-3}) upon addition of various concentrations of HBF$_4$ in CH$_3$OH [HBF$_4$]: $0-6.2 \times 10^{-5}$ mol dm^{-3}. Inset: the addition of KOH in CH$_3$OH solution to the solution of the acid titration [OH$^-$]: $0-7.0 \times 10^{-5}$ mol dm^{-3}.

Acid/Base-Controlled Molecular Switching On the basis of L^1. Upon titration of L^1 with HBF$_4$ as a proton source in CH$_3$OH, the absorption at about 360−375 nm steadily decreases and a concomitant absorption peak centered at 395 nm appears together with an isosbestic point at 378 nm. To validate a tentative assignment of the peaks in the absorption spectra, a geometry optimization was performed at the B3LYP/6-311+G* level (with the single-point energy and orbitals calculated at the TD-DFT-(B3LYP/6-311+G*) level) to determine the binding site of H$^+$ within L^1. The calculated total energies of the molecule in which H$^+$ was associated with O1, O2, N3, N4, and N5 are −1198.478435, −1198.478574, −1198.506804, −1198.519931, and −1198.532781 au, respectively (Scheme 1 and Supporting Information). The hydrogen ion associated with N5 on the naphthyrine moiety involves the promotion of the $\pi_{py} \rightarrow \pi^*_{napy}$ transition, leading to a longer wavelength absorption. This process is fully reversible by adding a base such as KOH in CH$_3$OH to the solution of the acid titration (Figure 7). In CH$_3$OH, L^1 exhibits an intensive emission with a λ_{max} at 407 nm upon excitation at 380 nm at room temperature. The luminescence intensity was measured as a function of HBF$_4$ concentration and decreased with an increase in the degree of protonated N atoms. The emission maximum was red-shifted from 407 to 440 nm with a low-energy emission band that tails beyond 630 nm at room temperature.

Photoinduced Isomerization. The photoinduced isomerization of L^1-L^3, **1**, **3**, and **4** was investigated at different excitation wavelengths. By irradiating L^1-L^3 in CH$_2$Cl$_2$, CH$_3$CN, or CH$_3$OH at 365 nm, the intensity of the absorption band around 370 nm decreased, but new bands emerged at 315 and 420 nm. Their absorption intensities developed as the irradiation times increased. These processes are characterized by isosbestic points at 330 and 392 nm. During the irradiation the emission band with a λ_{max} at about 405 nm rapidly weakened upon excitation at 330 nm. The spectral changes recorded during irradiation at room temperature are displayed in Figure 8. A comparison of the absorption spectra for complexes **1**, **3**, and **4** demonstrates that the mononuclear
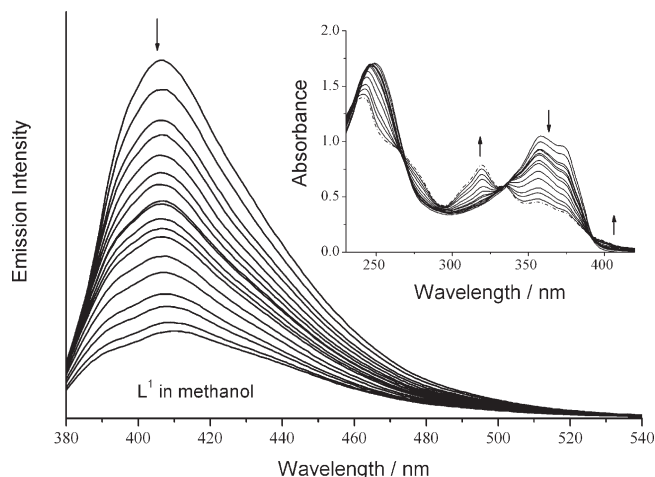
Figure 8. Emission spectra recorded during the irradiation of L^1 solution in CH₃OH at 365 nm upon excitation at 330 nm. Inset: changes in the absorption spectra.
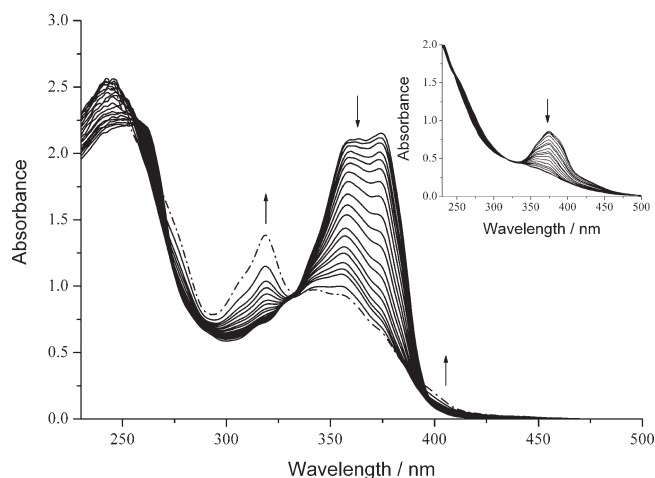

Figure 9. Absorption spectra recorded during the irradiation of complex **1** solution in CH₃OH at 365 nm. Inset: changes in the absorption spectra during the irradiation of complex **3** at 380 nm.

complex **1** has similar spectral behavior to ligand L^1 during irradiation at 365 nm, but in the case of **3** and **4** the new absorption bands were not observed. Moreover, the absorption peaks of **3** and **4** at 375 nm decreased in intensity (Figure 9). A geometry optimization was carried out for L^1 at the B3LYP/6-311+G* level to interpret the spectral properties (Supporting Information). The minimized energies for the *cis*- and *trans*-conformations were −1198.125283 and −1198.135446 au, respectively. The computational results showed that for the former conformation, a transition at 353.5 nm (3.508 eV, f = 0.123) is possible although the calculated lower-energy gap ($\Delta E_{\text{LUMO–HOMO}}$) of 3.201 eV is smaller than the 3.293 eV of the latter conformation. This indicates that a photoinduced isomerization reaction occurs from the *trans*- to cis-conformations after the irradiation of L^1 in solution.

In contrast to **1**, the spectral changes of **3** and **4** in the presence of light are best described as resulting from a structural distortion that causes a change in the natural ICT state because of the introduction of the bridging ligands, dppm, or dcpm, into the binuclear complexes to increase their rigidity.

Conclusions

We synthesized five novel flexible 1,8-naphthyridine derivatives containing vinyl and four mono- and dinuclear complexes. TD-DFT calculations and structural characterization of the compounds showed that groups around the C=C double bond adopt a stable *trans*-configuration. The hydrogen atom on the hydroxyl of L^3 can easily transfer to an adjacent naphthyridine-N atom resulting in a keto configuration. A structural investigation of L^4 revealed that two hydrogen atoms on the methyl at the 2-position of the naphthyridine or amino groups on pyridine can be substituted by acetyl groups in normal acetic anhydride and a 1,3-hydrogen transfer from the −CH− group of the β-diketone to an adjacent naphthyridine-N atom occurs during the formation of the compound. This leads to the formation of a pyrrolo[1′,5′-a]-1,8-naphthyridine derivative L^5 with promising visible absorption and red luminescence by the 1,5-dipolar cyclization of L^4 in anhydrous acetic anhydride. The calculations further demonstrated that the lower-energy absorption bands of L^1−L^3 come from an intramolecular $\pi_{\text{py}} \rightarrow \pi^*_{\text{napy}}$ charge transfer transition whereas those of L^4 and L^5 had opposite natural excited states. The dinuclear complexes exhibited two different MLCT characteristics that originated from the Cu-naphthyridine and Cu-pyridine moieties, and the excitation energy of the former is lower than that of the latter. The absorption spectra of L^1−L^3 show an acid/base-controlled molecular switching effect, and this process is reversible. The flexible compounds L^1−L^3 and **1** can undergo photoinduced isomerization in going from their t*rans*- to *cis*-conformations after solution irradiation, resulting in a red shift of their absorption spectra. These results provide new insights into the development of flexible 1,8-naphthyridine derivatives and their copper(I) complexes for potential application in medicine and materials science.

Supporting Information Available: X-ray crystallographic files in CIF format for L^{3-5} and complexes **1**−**4**; ¹H NMR of L^{1-5} and ¹³C NMR of L^4 and L^5; and computational details for TD-DFT are provided. This material is available free of charge via the Internet at http://pubs.acs.org.